



1 **Ozone and Aerosol Optical Depth Retrievals Using the Ultraviolet Multi-Filter Rotating**  
2 **Shadow-band Radiometer**

3  
4 Joseph Michalsky<sup>1</sup> and Glen McConville<sup>1,2</sup>

5  
6 <sup>1</sup>Global Monitoring Laboratory, National Oceanic and Atmospheric Administration,  
7 325 Broadway, Boulder, Colorado 80305 USA

8 <sup>2</sup>Cooperative Institute for Research in Environmental Sciences, University of Colorado,  
9 216 UCB, Boulder, Colorado 80309 USA

10  
11 *Correspondence to:* Joseph Michalsky (joseph.michalsky@noaa.gov)

12  
13  
14 **Abstract:** The ultraviolet multi-filter rotating shadowband radiometer (UV-MFRSR) is a seven-  
15 channel radiometer with narrowband filters centered between wavelengths 300 and 368 nm. Four  
16 of the middle wavelengths in this device are near those used in the Dobson spectrometer to  
17 retrieve ozone column abundance. In this paper measurements from Mauna Loa Observatory  
18 (MLO) were used, first, to calibrate the instrument using the Langley plot method, and,  
19 subsequently, to derive column ozone and aerosol optical depths. The ozone derived from the  
20 UV-MFRSR was compared to the ozone measured by a Dobson spectrophotometer that operates  
21 daily at the MLO resulting in column values within about 1 DU on average for 43 days in 2018.  
22 The aerosol optical depth (AOD) retrievals are more challenging. Generally, the AOD increases  
23 with wavelength between 305 and 332 nm; not what is expected given the typical AOD  
24 wavelength dependence at visible wavelengths. An example of this behavior is discussed, and  
25 research by others is cited that indicates similar behavior at these wavelengths, at least for the  
26 low aerosol optical depth conditions encountered at high altitude sites.

27  
28  
29 **Introduction**

30  
31 Most historical network measurements of column ozone from the surface used Dobson or  
32 Brewer spectrometers, and these continue as the predominant ozone measurement instruments  
33 today. Brief explanations of these two devices and comparisons of concurrent and collocated  
34 measurements of total column ozone are given in Staehelin et al. (2003). Gao et al. (2001)  
35 demonstrated that ozone could be retrieved using the ultraviolet multi-filter rotating shadow-  
36 band radiometer (UV-MFRSR), which agreed with those values retrieved from either collocated  
37 Dobson and/or Brewer spectrophotometers to within 1-2%.

38  
39 The wavelengths used for ozone retrievals in the UV-MFRSR more closely match wavelengths  
40 in the Dobson rather than the Brewer spectrophotometer. Typically, ozone retrieved from the  
41 Dobson uses the AD wavelength pairs ‘A’ 305.5/325.4 and ‘D’ 317.6/339.8. Since there is no  
42 filter near 339.8 nm, the UV-MFRSR uses filters near the ‘A’ pair and the Dobson ‘C’ pair  
43 311.5/332.4. The filters in the UV-MFRSR that are used for ozone measurements are nominally  
44 the 305/325 nm pair and the 311/332 nm pair with carefully measured profiles of these filters  
45 used for actual retrievals.

46



47 The basic procedure consists of measuring extinction at two wavelengths with one chosen to be  
48 more strongly attenuated than the other in the Hartley-Huggins ultraviolet bands. The basic  
49 extinction equation can be written

50

$$I(\lambda) = I_0(\lambda) \cdot \exp [-\tau_{ray}(\lambda)m_{ray}(\lambda) \left(\frac{P}{P_0}\right) - \tau_{oz}(\lambda)m_{oz}(\lambda) - \tau_{aer}(\lambda)m_{aer}(\lambda)] \quad (1)$$

51

52 or, equivalently,

53

$$V(\lambda) = V_0(\lambda) \cdot \exp [-\tau_{ray}(\lambda)m_{ray}(\lambda) \left(\frac{P}{P_0}\right) - \tau_{oz}(\lambda)m_{oz}(\lambda) - \tau_{aer}(\lambda)m_{aer}(\lambda)] \quad (2)$$

54 since the ratios  $I/I_0$  and  $V/V_0$  are equal.

55

In these equations:

$I(\lambda)$  = spectral irradiance measured by the instrument at the surface

$I_0(\lambda)$  = spectral irradiance measured by the instrument at the top of the atmosphere

$V(\lambda)$  = signal (voltage) measured by the instrument at the surface

$V_0(\lambda)$  = signal (voltage) measured by the instrument at the top of the atmosphere

$\tau$ 's = optical depths for Rayleigh scattering (ray), ozone (oz), and aerosol (aer)

P,  $P_0$  = atmospheric pressure at the measurement site and at sea level, respectively

$m$ 's = airmasses for Rayleigh, ozone, and aerosol relative to a vertical path; they differ slightly because each has a different distribution with altitude in the atmosphere.

56 If we write ozone optical depth as  $\tau_{oz} = \alpha_{oz} \cdot \eta_{oz}$ , where  $\alpha_{oz}$  is the ozone absorption coefficient  
57 and  $\eta_{oz}$  is the abundance of ozone, we can solve for  $\eta_{oz}$  by rearranging terms in two versions of  
58 eqn. (2) representing the two wavelengths in the pair (the longer wavelength is indicated by  
59 primes). Therefore, dropping the explicit  $\lambda$  dependence for clarity, we get for ozone abundance  
60

$$\eta_{oz} = \frac{N - (\tau_{ray} - \tau'_{ray})m_{ray} \left(\frac{P}{P_0}\right) - (\tau_{aer} - \tau'_{aer})m_{aer}}{(\alpha_{oz} - \alpha'_{oz})m_{oz}}, \quad (3)$$

61

62

63 where N is defined as

64

$$N = \ln \left( \frac{V_0}{V_0'} \right) - \ln \left( \frac{V}{V'} \right).$$

65

66 Since all of the parameters of eqn. (3) are known or can be calculated, one could solve for  $\eta_{oz}$  if  
67 the term  $(\tau_{aer} - \tau'_{aer})$ , i.e., the aerosol optical depths at the two wavelengths were known. To  
68 curtail this requirement, the 'A' and 'C' wavelength pairs are used, and the assumption is made  
69 that since the wavelength separation of each pair is nearly the same and the wavelength  
70 dependence over this small wavelength region is expected to be nearly linear, subtraction of eqn.  
71 (3) applied to each pair will come very close to eliminating the aerosol terms because subtraction



72 of aerosol terms should be near zero if these assumptions hold. The resulting equation used to  
73 calculate ozone is  
74

$$\eta_{oz} = \frac{N_1 - N_2 - [(\tau_{ray} - \tau'_{ray})_1 - (\tau_{ray} - \tau'_{ray})_2]m_{ray}(P/P_o)}{[(\alpha_{oz} - \alpha'_{oz})_1 - (\alpha_{oz} - \alpha'_{oz})_2]m_{oz}}, \quad (4)$$

75  
76  
77 where

$$N_1 = \ln\left(\frac{V_{o,305}}{V'_{o,325}}\right) - \ln\left(\frac{V_{305}}{V'_{325}}\right),$$

79  
80 and

$$N_2 = \ln\left(\frac{V_{o,311}}{V'_{o,332}}\right) - \ln\left(\frac{V_{311}}{V'_{332}}\right).$$

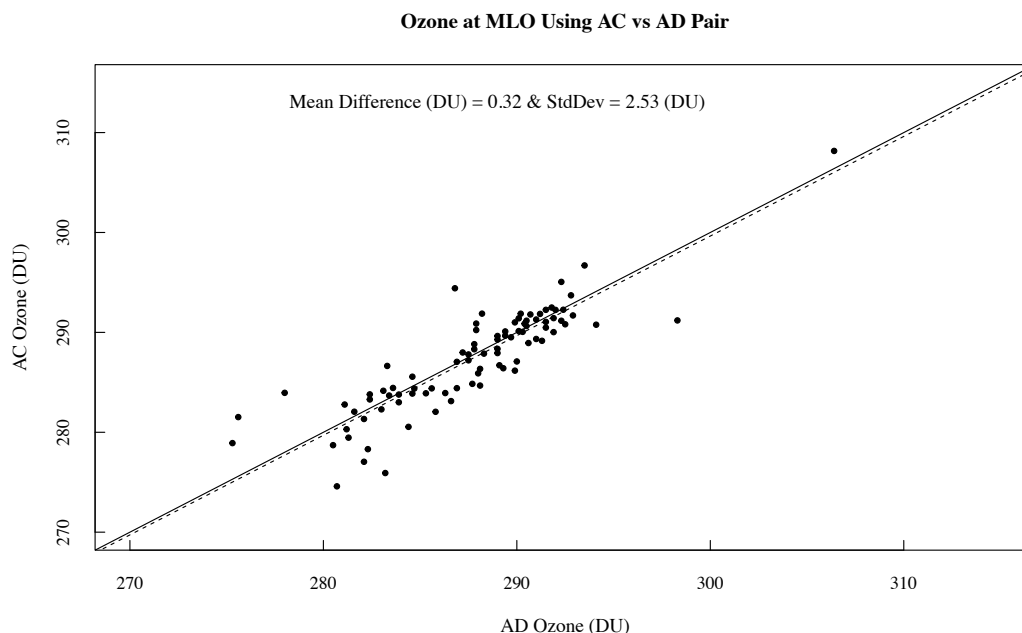
### 85 Calibration and Ozone Measurement Comparisons

86  
87 The Langley calibration of the UV-MFRSR was performed at NOAA's Mauna Loa Observatory  
88 (Latitude = 19.5362°N; Longitude = 155.5763°W; 3397 m). The height of the observatory often  
89 allows measurements to be made in clean, free-tropospheric air above the marine boundary layer,  
90 especially in the morning hours.

91  
92 UV-MFRSR data were obtained on 242 days in 2018 beginning on 14 February and ending on  
93 15 October. There were 139 successful Langleys during this period that produced estimated  $V_o$ 's  
94 with only 27 of these during the afternoon hours. Looking at the retrieved  $V_o$ 's as a function of  
95 time there is a hint of a decrease, but not one filter indicates a statistically significant decline,  
96 therefore, averages of  $V_o$ 's over the entire period are used in the ozone and aerosol retrievals.

97  
98 Ozone is a standard measurement at NOAA's Mauna Loa Observatory and has been made with  
99 near continuous sampling since 1963. The Dobson spectrophotometer makes AD paired  
100 measurements to determine ozone using absorption coefficients measured by Bass and Paur  
101 (1985). No estimate of the ozone column below the observatory, which could be on the order of  
102 5% of the column total at sea level, is made. Therefore, the column measurements made using  
103 the UV-MFRSR can be directly compared to the Dobson column measurements if one uses the  
104 Bass and Paur (1985) absorption cross-sections for the UV-MFRSR channels.

105  
106 Since the Dobson generally uses the AD pair for the total column ozone calculation, we  
107 investigated the difference between AC and AD Dobson retrievals on two clear days at Mauna  
108 Loa that were used for Langley calibrations of the Dobson thus giving us more than the  
109 operational 1000, 1200, and 1400 local time ozone measurements. It is important to assess any  
110 differences since the UV-MFRSR uses wavelengths close to the AC pair for its ozone retrievals.  
111 Figure 1 illustrates the difference between Dobson measurements with the two different



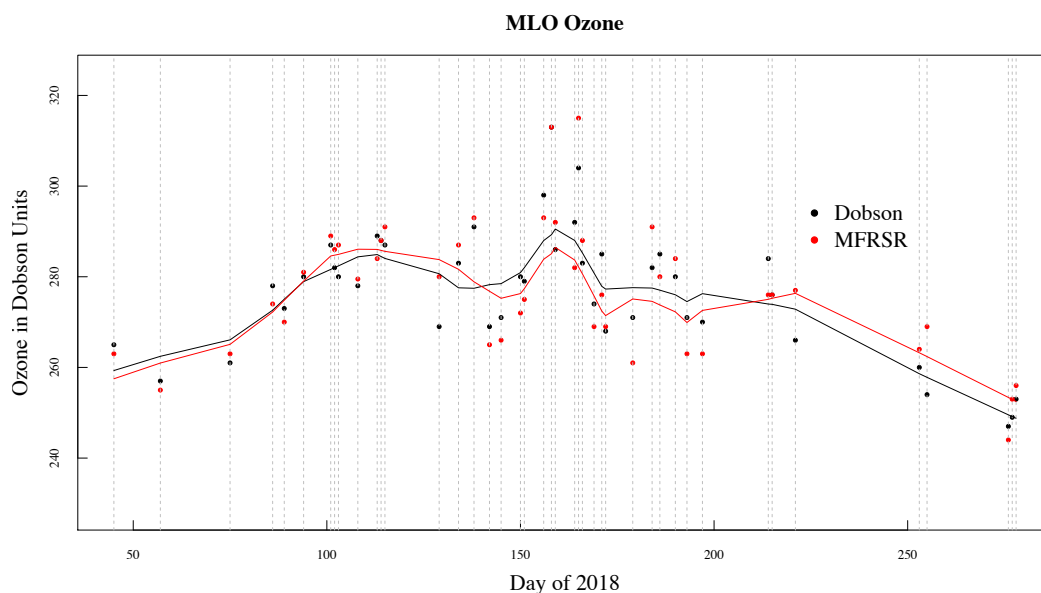
112  
113 **Figure 1. Plot of ozone measured by a Dobson unit at Mauna Loa Observatory retrieved using the Dobson**  
114 **AC pair versus the Dobson AD pair. Solid diagonal line is 1:1 line and dashed line is linear least-squares fit.**  
115 **The mean difference and standard deviation of the samples are given on the plot.**  
116

117  
118 wavelength pairs. The mean difference in retrieved ozone for the 90 points compared in the plot  
119 is less than 0.5 DU and the standard deviation among the 90 samples is close to 2.5 DU.  
120 Therefore, using the AC pair of the UV-MFRSR for ozone retrievals and comparing to AD-pair  
121 Dobson ozone should be acceptable.  
122

123 Figure 2 is a plot of the ozone time series retrieved from the Dobson AD pair and the UV-  
124 MFRSR AC pair for the 2018 data that were matched by day of year. In the case of the Dobson,



125 one measurement is chosen from the three daily measurements made at 1000, 1200 and 1400



126  
127 **Figure 2.** Time series plot of Mauna Loa Observatory for 43 days of retrieved ozone for 2018 using the  
128 **Dobson spectrophotometer (black dots) and the UV-MFRSR (red dots).** The lines are lowess fits using 0.25 of  
129 **the points for the lowess fit at each point. The Dobson uses one of three measured points for the daily value,**  
130 **and the UV-MFRSR uses the median of all 20-second, clear-sun data for air masses less than three.**

131  
132

133 local standard time. Only direct sun measurements made with the Dobson are used for this  
134 comparison. For the UV-MFRSR data, which is sampled every 20 seconds, a median value of all  
135 points, which are made at less than three air masses and that pass cloud-screening, is used. Since  
136 measurements from the two instruments are made differently and no attempt to make them  
137 coincident, except for occurring on the same day, there is no expectation of perfect agreement  
138 given any diurnal variability. The average difference over the 43-day sample is about 0.10  
139 Dobson units. The lowess fits to the two data sets track each other rather closely matching dips  
140 and peaks throughout the measurement period.

141  
142

### 143 Sources of Uncertainty

144

145 Uncertainties in using a UV-MFRSR for ozone retrievals were discussed thoroughly by Gao et  
146 al. (2001). In this paper only data taken at less than three air masses (about 71° solar-zenith  
147 angle) were used because (1) air mass determination is less certain at higher solar-zenith angles  
148 and the cosine response correction for the UV-MFRSR is larger and more difficult to pinpoint  
149 and, therefore, more uncertain. The extraterrestrial responses for the four filters used to retrieve  
150 ozone were averages for the 242-day period in 2018 as stated earlier. The uncertainties in  
151 extraterrestrial responses were between 0.2% and 0.3%. The ozone absorption coefficients were  
152 those measured by Bass and Paur (1985) adjusted for mid-latitude seasonal variations. The  
153 effective absorption coefficients were weighted by each of the four filter profiles, as were the



154 Rayleigh scattering optical depths. The Rayleigh optical depths were pressure corrected using  
155 on-site measurements of atmospheric pressure.

156  
157 Always a major concern when working in the ultraviolet is light from outside the band passes  
158 contributing to the measured signal. Si-C (silicon carbide) is the detector for the 300 nm and 305  
159 nm filters. GaP (gallium phosphide) is used as the detector in the five longest wavelength filters.  
160 To measure the extent of the possible long-wavelength leakage, we used a Schott glass OG530  
161 placed over the entrance optic being careful to block light paths from the edges that might reach  
162 the entrance diffuser optic. The transmission below 460 nm is 0.00001, therefore no light should  
163 reach the detectors with the OG530 completely covering the entrance optic. If higher orders of  
164 light from the interference filters would reach the detectors, they would begin to be a problem  
165 around 600 nm for the 300-nm filter and at longer wavelengths for the other six filters. The  
166 nighttime dark readings and 530 Schott blocking filter readings on a clear, sunny day were  
167 compared. These readings agreed within the detection limit for the UV-MFRSR.

168  
169

#### 170 **Aerosol optical depth retrievals**

171

172 After subtracting the large ozone and Rayleigh optical depth contributions to the total optical  
173 depth, a residual remains that is assumed to be aerosol extinction. Historically, at Mauna Loa the  
174 aerosol optical depths (AODs) are, in most cases, very small in the visible except in the  
175 aftermath of volcanic eruptions (Dutton et al., 1994). The current paper examines AODs in the  
176 ultraviolet at 305.6, 311.4, 317.5, 325.2, 332.4, and 367.8 nm where measurements of AOD are  
177 infrequently made. These wavelengths are shorter than those measured by most sunphotometers  
178 except for the 368 nm wavelength.

179

180 Figure 3 is typical of the AOD versus wavelength plots from the 43 days of measurements  
181 plotted in Fig. 2. *Typical visible* wavelength dependent behavior indicates a negative slope on  
182 this type of plot, however, the slope is positive from 305 to 332 nm and then becomes negative  
183 after that, with the 368-nm wavelength AOD smaller than the 332-nm wavelength. A careful  
184 search for systematic errors in a paper by Carlund et al. (2017) that examines another  
185 narrowband filter instrument for the ultraviolet did not explain the similar wavelength  
186 dependence (see the right-hand-side of their Fig. 6) that they measured for low aerosol optical  
187 depth days in Davos, Switzerland.

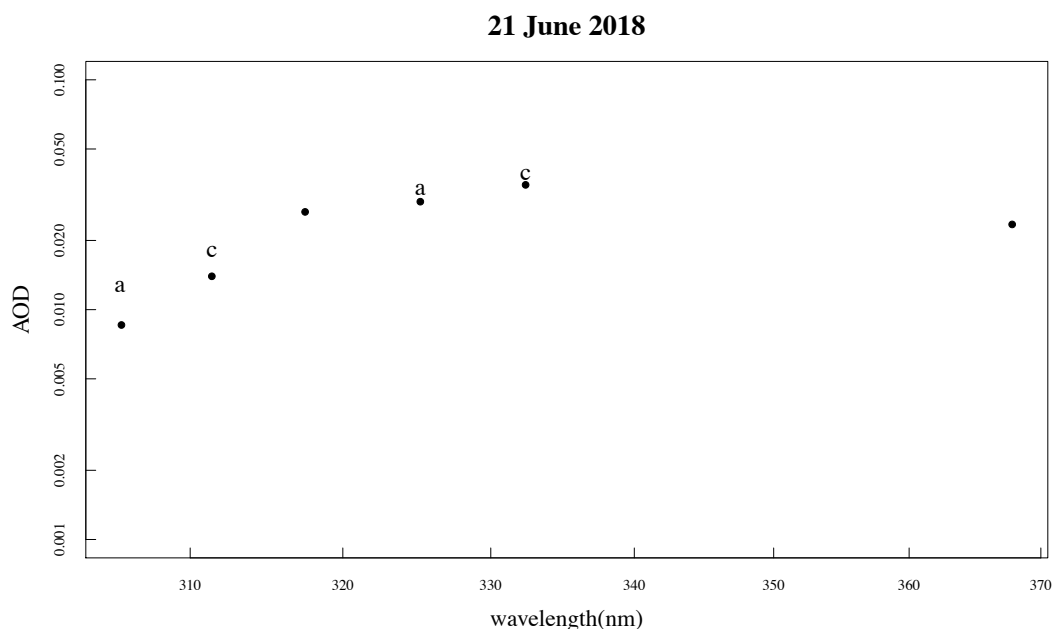
188

189 We also looked at nitrogen dioxide (NO<sub>2</sub>) as a possible contaminant that if not removed could  
190 explain this wavelength behavior, however, the typical amount of NO<sub>2</sub> in the column above  
191 Mauna Loa would necessitate a correction of less than 0.001 optical depths at 332 nm, less at the  
192 shorter wavelengths, and slightly more at 368 nm. When only considering the 332 nm and 368  
193 aerosol optical depths the plot indicates the typical visible wavelength dependence. Although  
194 Fig. 3 is the only plot of AOD shown, all of the 43 days showed similar behavior.

195

196

197



198  
199  
200  
201  
202  
203  
204  
205  
206  
207  
208  
209  
210  
211  
212  
213  
214  
215  
216  
217  
218  
219  
220  
221  
222  
223

**Figure 3.** This plot indicates the AOD versus wavelength for the UV-MFRSR filter set at Mauna Loa Observatory. Instead of a negative slope, this figure, which is typical of the 43 days in this study, indicates a positive slope with a negative slope indicated only by the two longest wavelengths. The ‘a’ and ‘c’ labels are included to indicate the wavelength pairs used for the ozone retrievals.

## Discussion

This paper focuses on data from the Manua Loa Observatory only. It corroborates results reported by Gao et al. (2001) regarding the UV-MFRSR’s ability to retrieve ozone column that is in agreement with the Dobson instrument at Mauna Loa Observatory. Figure 2 demonstrates this agreement even though there was no attempt to synchronize ozone observations other than to have them occur on the same day.

Aerosol optical depths were measured in this very clean environment with expected low values, but an unexpected wavelength dependence. This wavelength dependence is similar to that obtained with an independent, sun-pointed narrowband filter instrument developed and operated at the World Radiation Center (WRC) in Davos, Switzerland. Our and the WRC’s attempts to explain this wavelength dependence have yet to yield an understanding of the physics at work here. Systematic biases may be responsible; a better understanding of the very large optical depths associated with ozone absorption and Rayleigh scattering at these wavelengths that have to be subtracted to obtain the small AOD at these wavelengths may require more investigation. On the other hand, further study of environments with somewhat larger aerosol optical depths may indicate that this is, perhaps, associated with aerosol size distributions in some conditions.



224 *Author contributions:* JM drafted the paper and produced the figures. GM produced the data for  
225 Fig. 1 and provided details about the Dobson ozone retrievals using the AD and AC pairs.

226

227 *Competing interests.* The contact author has declared that none of the authors has any competing  
228 interests.

229

230 *Acknowledgments.* This paper benefited from Dobson ozone retrieval discussions with Peter  
231 Effertz and Irina Petropavlovskikh. Kathy Lantz provided the UV-MFRSR data from Mauna Loa  
232 Observatory and performed the out-of-band rejection studies. She also provided a critical reading  
233 of the draft paper. Thomas Carlund provided useful insight on WRC's efforts at ultraviolet AOD  
234 retrievals using the World Radiation Center (WRC) UV-PFR while he was on sabbatical at the  
235 WRC in Davos, Switzerland.

236

237 *Financial support.* The publication costs for this paper were covered by the Global Monitoring  
238 Laboratory of the National Oceanic and Atmospheric Administration.

239

240

## 241 **References**

242

243 Bass, A. M. and Paur, R. J. 1985: The ultraviolet cross sections of ozone: I. The measurements.  
244 In *Atmospheric Ozone - Proceedings of the Quadrennial Ozone Symposium 1984*, (Editors: C.S.  
245 Zerefos and A. Ghazi), pp. 606-610, Springer, Dordrecht. [https://doi.org/10.1007/978-94-009-5313-0\\_120](https://doi.org/10.1007/978-94-009-5313-0_120), 1985.

246

247  
248 Carlund, T., Kouremeti, N., Kazadzis, S., and Gröbner, J.: Optical depth determination in the UV  
249 using a four-channel precision filter radiometer. *Atmos. Meas. Tech.*, 10, 905-923,  
250 [doi:10.5194/amt-10-905-2017](https://doi.org/10.5194/amt-10-905-2017), 2017.

251

252 Dutton, E. G., Reddy, P., Ryan, S., and DeLuisi, J. J.: Features and effects of aerosol optical  
253 depth observed at Mauna Loa, Hawaii: 1982-1992. *J. Geophys. Res.*, 99, 8295-8306,  
254 [doi.org/10.1029/93JD03520](https://doi.org/10.1029/93JD03520), 1994.

255

256 Gao, W., Slusser, J., Gibson, J., Scott, G., Bigelow, D., Kerr, J. and McArthur, B.: Direct-Sun  
257 column ozone retrieval by the ultraviolet multifilter rotating shadow-band radiometer and  
258 comparisons with Brewer and Dobson spectrophotometers. *Appl. Optics*, 40, 3149-3155, [doi:  
259 10.1364/AO.40.003149](https://doi.org/10.1364/AO.40.003149), 2001.

260

261 Staehelin, J., Kerr, J., Evans, R. and Vanicek, K., Comparison of total ozone measurements of  
262 Dobson and Brewer spectrophotometers and recommended transfer functions, WMO/GAW 149  
263 (WMO TD 1147), 39 pp., 2003.

264